3.10 SUPPLEMENT ON CHEMICAL BONDING

(SCF, LCAO, MO's and CO's*)

sections:

A more detailed and advanced treatment of SCF calculations, and of the LCAO approach to molecular orbitals and chemical bonding, can be found in the following texts:

R. McWeeney, Coulson's Valence, 3rd Ed., Oxford U. Press (1979).

J. N. Murrell et al, The Chemical Bond, 2nd Ed., Wiley & Sons (1985).

J. C. Slater, Quantum Theory of Matter, McGraw-Hill (1951).

More elementary and pictorial treatments appear in:

H. B. Gray, Chemical Bonds: An Introduction to Atomic and Molecular Structure, Benjamin (1973).

G. C. Pimentel and R. D. Spratley, Chemical Bonding Clarified Through Quantum Mechanics, Holden-Day (1969).

---

* Warning: Too much CO is hazardous to your health.

THE VARIATION METHOD

Solving Schrödinger's equation for multi-electron atoms was hard enough, but was simplified by Hartree's assumption that the potential V for each electron was spherically symmetric, the so-called central-field model. However, this assumption is no longer feasible even for the simplest molecule, so another approach is required to find approximate solutions to Schrödinger's equation for molecules. The most commonly-used approach to obtain molecular orbitals is to construct them as linear combinations of atomic orbitals (LCAO). The LCAO method is a special case of a more general method used to find approximate solutions to Schrödinger's equation, the variation method (also known as the Rayleigh-Ritz method).

If we take the Schrödinger equation $H\psi = E\psi$, multiply both sides by ψ (or ψ^* if ψ is complex), and integrate over all the coordinates involved ($d\tau$), we get:

$$\int \psi H \psi \, d\tau = E \int \psi^2 \, d\tau$$

Clearly, if the ψ we have chosen are solutions for this particular H, the ratio

$$\mathcal{E}(\psi) = \frac{\int \psi H \psi \, d\tau}{\int \psi^2 \, d\tau}$$

will equal the associated energy E. However, if we don't know the proper wave functions, the variation theorem states that for any trial wave function ψ,

$$\mathcal{E}(\psi) \geq E$$

The best choice for ψ will be the one that gives the lowest value of $\mathcal{E}(\psi)$. The general approach, therefore, is to assume a reasonable form of ψ with several parameters C_1, C_2, etc., and adjust these parameters to minimize $\mathcal{E}(\psi)$.

As a simple example, we could make the wise guess of $\psi = e^{-cr}$ as a solution to Schrödinger's equation for the hydrogen atom, for which

$$H = -\frac{\hbar^2}{2m}\nabla^2 - \frac{e^2}{4\pi\epsilon_0 r}$$

Plugging the assumed ψ into the above integrals, and minimizing $\mathcal{E}(\psi)$ with respect to c will yield

$$c = \frac{me^2}{4\pi\epsilon_0\hbar^2} = \frac{1}{a_0} \qquad \text{and} \qquad \mathcal{E}_{min} = \frac{-me^4}{2(4\pi\epsilon_0)^2\hbar^2} = 13.6\ eV$$

where a_0 is the Bohr radius. In this case, our "lucky" guess for ψ actually gave the true ground-state ψ and E. If we had instead guessed $\psi = \exp(-cr^2)$, our $\mathcal{E}_{min}$ would have been 15% higher than the true value. If we had guessed $\psi = \exp(-c_1 r^2) + k\exp(-c_2 r^2)$, with C_1, C_2, and k all variable parameters, the error would have been reduced to 1.3%. The use of more parameters will generally add to the accuracy, but also add to the length of the calculations, so some compromise between accuracy and convenience is usually necessary.

LCAO - THE HYDROGEN MOLECULAR ION

A particular application of the variation method to molecular orbitals (MO's) of a diatomic molecule is to assume them of the form

$$\psi = c_1 \phi_1 + c_2 \phi_2$$

where ϕ_1 is an atomic orbital (AO) centered on atom 1 and ϕ_2 is an AO centered on atom 2. Thus ψ is formed as a linear combination of atomic orbitals (LCAO).

To be more specific, we consider the simplest of all diatomic systems - the hydrogen molecular ion H_2^+, which consists of two protons (separated by distance R) and only one electron. Since the protons are much heavier and much slower than the electron, we assume that R is fixed as we try to solve Schrödinger's equation for the electron in its potential energy field V, where

$$V = \frac{-e^2}{4\pi\epsilon_0}\left(\frac{1}{r_1} + \frac{1}{r_2}\right)$$

and r_1 and r_2 are the distances of the electron from nuclei 1 and 2, respectively.

For AO's, we choose the 1s normalized orbitals centered on each of the nuclei:

$$\phi_1 = \frac{1}{\sqrt{\pi a_0^3}} e^{-r_1/a_0} \quad \text{and} \quad \phi_2 = \frac{1}{\sqrt{\pi a_0^3}} e^{-r_2/a_0}$$

We then plug $\psi = c_1\phi_1 + c_2\phi_2$ into the expression for $\mathcal{E}(\psi)$ given in the previous section. Since ϕ_1 and ϕ_2 are normalized, $\int \phi_1^2 d\tau = \int \phi_2^2 d\tau \equiv 1$, and the denominator in $\mathcal{E}(\psi)$ becomes

$$\int \psi^2 d\tau = c_1^2 + c_2^2 + 2 c_1 c_2 \int \phi_1 \phi_2 d\tau$$

The integral in the third term is important enough to warrant a name, the overlap integral:

$$S_{12} = \int \phi_1 \phi_2 d\tau$$

(The integrand is small unless both ϕ_1 and ϕ_2 are fairly large, i.e., where they overlap.)

The numerator in $\mathcal{E}(\psi)$ contains three integrals (reduced from four by the symmetry property $\int \phi_1 H \phi_2 d\tau = \int \phi_2 H \phi_1 d\tau$):

$$\int \psi H \psi d\tau = c_1^2 \int \phi_1 H \phi_1 d\tau + c_2^2 \int \phi_2 H \phi_2 d\tau + 2 c_1 c_2 \int \phi_1 H \phi_2 d\tau$$

The first two integrals, since V contains only terms representing the Coulomb attraction between the electron and each of the nuclei, are called Coulomb integrals

$$H_{11} = \int \phi_1 H \phi_1 d\tau \quad \text{and} \quad H_{22} = \int \phi_2 H \phi_2 d\tau$$

The final integral is known as the bond integral:

$$H_{12} = \int \phi_1 H \phi_2 d\tau$$

Using these symbols for the various integrals, our full expression for $\mathcal{E}$ therefore becomes:

$$\mathcal{E}(\psi) = \frac{c_1^2 H_{11} + c_2^2 H_{22} + 2 c_1 c_2 H_{12}}{c_1^2 + c_2^2 + 2 c_1 c_2 S_{12}}$$

Applying the variation method, as described earlier, involves setting $\partial\mathcal{E}/\partial c_1 = \partial\mathcal{E}/\partial c_2 = 0$. After a little algebra, this yields what are called the secular equations:

$$c_1(H_{11}-E) + c_2(H_{12}-ES_{12}) = 0$$
$$c_1(H_{12}-ES_{12}) + c_2(H_{22}-E) = 0$$

(We have now replaced $\mathcal{E}$ with E because for these values of C_1 and C_2, $\mathcal{E}$ is the closest approximation to the true energy E.) These secular equations are then solved to determine values for E and the corresponding values of the ratio C_2/C_1. With two secular equations, we will have two solutions. Had we started with a trial wave function in the form of a linear combination of n AO's, we would have generated a set of n secular equations with n solutions, corresponding to n energy levels.

In our particular case, since H_2^+ has two identical nuclei (is homonuclear), $H_{11}=H_{22}=H$ by symmetry. The two secular equations then yield:

$$(H-E)^2 = (H_{12}-ES_{12})^2$$

which has two solutions:

$$E = \frac{H+H_{12}}{1+S_{12}} \quad \text{and} \quad E = \frac{H-H_{12}}{1-S_{12}}$$

which can be rewritten as:

$$E = H + \frac{H_{12}-HS_{12}}{1+S_{12}} \quad \text{and} \quad E = H - \frac{H_{12}-HS_{12}}{1-S_{12}}$$

anti bond

At large R, $S_{12}=H_{12}=0$ (no overlap, no coupling, no bonding), and E=H. The reference state for large R is a separated H and H^+. As R decreases, overlap and coupling increase, and the original pair of degenerate levels of energy H is split into two, one lying below and one lying above the original level (Fig. 6). (See S&W 5.8 for an alternate description of this splitting.)

The splitting of the energy levels is dominated by the bond integral H_{12}. The lower energy level, on the left above, corresponds to $C_1=C_2$, a bonding MO produced by adding the two AO's. The higher energy level corresponds to $C_1=-C_2$, an anti-bonding MO produced by subtraction. Figure 7 schematically shows the formation of these two MO's from the two AO's by showing the amplitude of the MO's (solid lines) and AO's (dashed lines) along the line through the two nuclei. The bonding MO is symmetric, the anti-bonding MO anti-symmetric. Contours showing the electron density distribution of the two MO's are seen in Fig. 8. The bonding MO has a substantial electron density between the two nuclei, while the anti-bonding MO has a nodal plane between the nuclei. The bonding and anti-bonding MO's are traditionally labeled $1\sigma_g$ and $1\sigma_u^*$, following a system that will be explained a bit later.

$E_t(R)$

The total energy of H_2^+ will consist of the electronic energy as calculated above plus a term $e^2/4\pi\epsilon_0 R$ representing the repulsion between the two nuclei. The total molecular energy for the case of the bonding MO has a minimum with respect to R, while that for the anti-bonding MO does not (Fig. 9). Thus the former represents a stable molecule and the latter does not. If the calculation is carried through with the specific AO's used above, the interatomic spacing and binding energy that emerge are only in rough agreement with experiment. A slightly improved calculation, using more parameters, yields essential agreement (Fig. 10a).

If we add a second electron to our two-proton system, we have the neutral H_2 molecule. We must then account for the repulsion between the electrons by the SCF method discussed earlier, but we end up with very similar results. In the ground state, the two electrons (with opposite spin) will both occupy the energy level corresponding to the bonding MO. The equilibrium interatomic distance decreases, and the bonding energy increases (Fig. 10b). Now two electrons preferentially occupy the space between the two protons, providing the "glue" of the covalent bond that holds the molecule together. This concentration of electrons between the nuclei is shown in Fig. 11, which shows contours of the "difference density", i.e., the difference between the electron density of the bonding MO and the densities of two non-bonded hydrogen atoms located at the positions of the nuclei.

Such LCAO calculations yield several results that can be compared with experiment - the bonding energy, the interatomic spacing, and the energy gap between the ground state ($1\sigma_g$) and the first excited state ($1\sigma_u^*$), a gap that is observable spectroscopically. Another important property is related to the curvature of the $E_t(R)$ curve at the equilibrium spacing, which determines the energy required to change the bond length (Fig. 12). By analogy to two particles joined by a spring, the force constant (or "spring" constant) influences the frequencies and energies of molecular vibrations.

In determining the electron distribution in the molecules, we considered the nuclei stationary because they are much heavier, and therefore slower, than the electrons. However, the nuclei in all molecules do vibrate about their equilibrium positions, and vibrational energy levels are quantized, just like electronic energy levels. The associated transitions are generally of much lower energy, and usually correspond to the far infrared.

Molecular vibrational energies and frequencies are determined by the masses of the nuclei and by the force constant. The force constant is proportional to $\partial^2 E_t/\partial R^2$ at the equilibrium distance, and is determined, as is the equilibrium distance, by a balance between the attractive and repulsive components of the interatomic forces. Increased bonding energies generally are associated both with decreased interatomic distances ("bond lengths") and with increased force constants.

As in molecules, the interatomic distances in solids are determined by a balance between attractive and repulsive forces. The interatomic force constants in solids are proportional to an analogous $\partial^2 E_t/\partial R^2$, and determine the frequencies of atomic vibrations in the solids. The quantized lattice vibrations in solids, known as phonons, play an important role in determining specific heat, thermal conductivity, superconductivity and some aspects of spectroscopy. The force constants also directly determine mechanical properties such as the bulk elastic modulus, as described in S&W 5.2 .

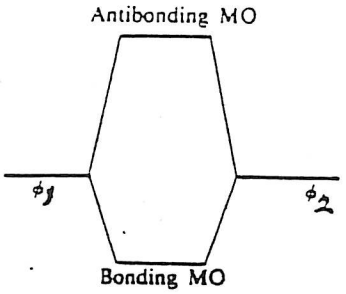

FIG. 6 Energy level diagram for molecular orbital formation. The energy of an electron in the bonding MO is *lower* than in the original AO (ϕ_1 or ϕ_2); for the antibonding MO it is higher.

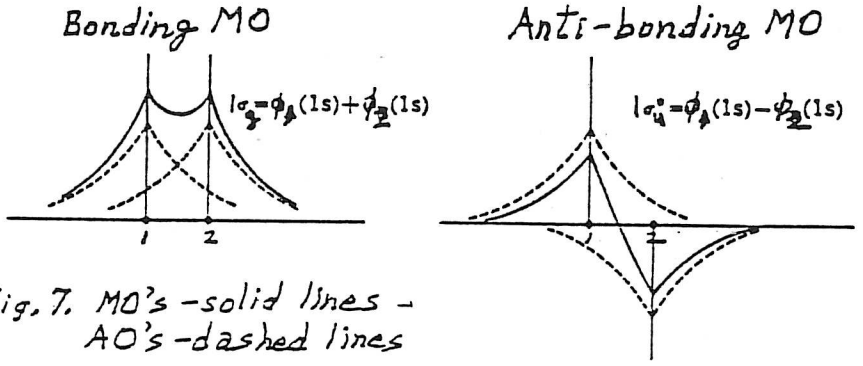

Fig. 7. MO's - solid lines - AO's - dashed lines

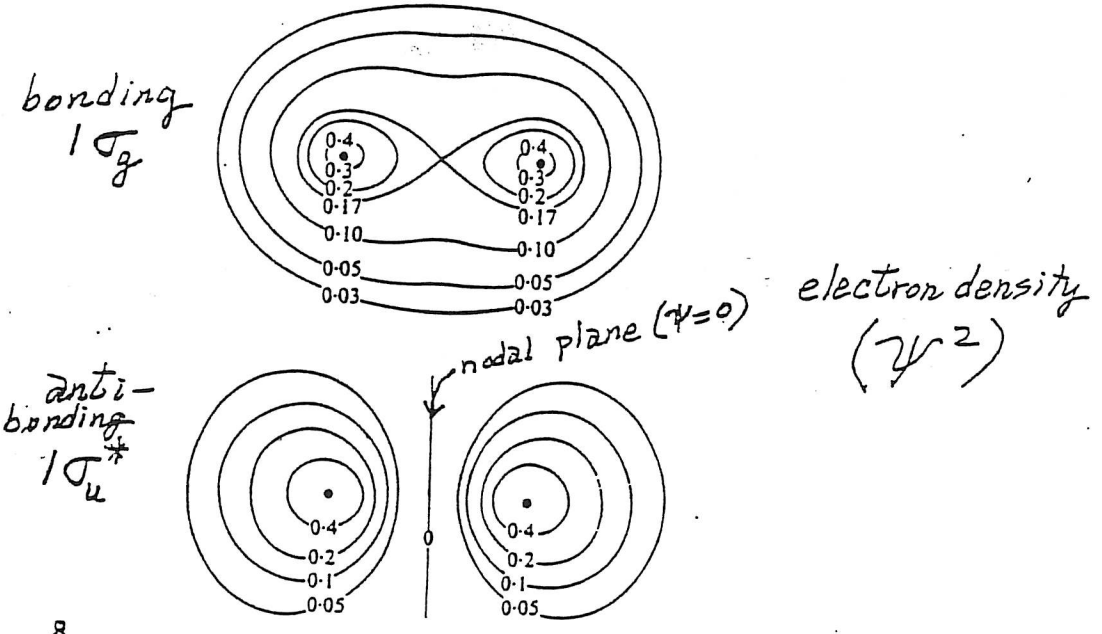

FIG. 8 Electron density in the ion H_2^+. The upper diagram is for the electron in the bonding MO, and the lower diagrams is for the antibonding MO ($1\sigma_g$ and $1\sigma_u^*$ are the conventional names of these MO's).

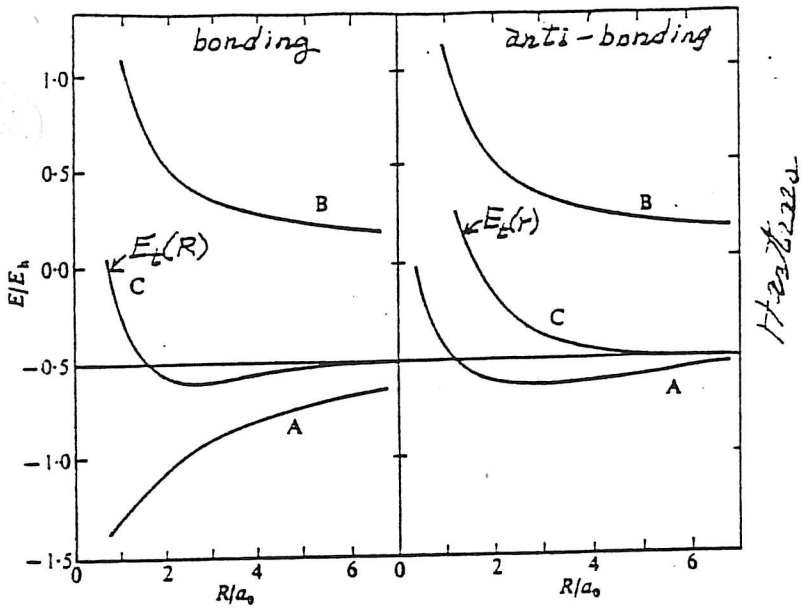

FIG. 9 Energy curves for the ion H_2^+. The left-hand diagram is for the bonding MO, and the right-hand diagram for the antibonding MO: curves A, purely electronic energy; curves B, nuclear repulsion energy; curves C, resultant energy curve of the molecule.

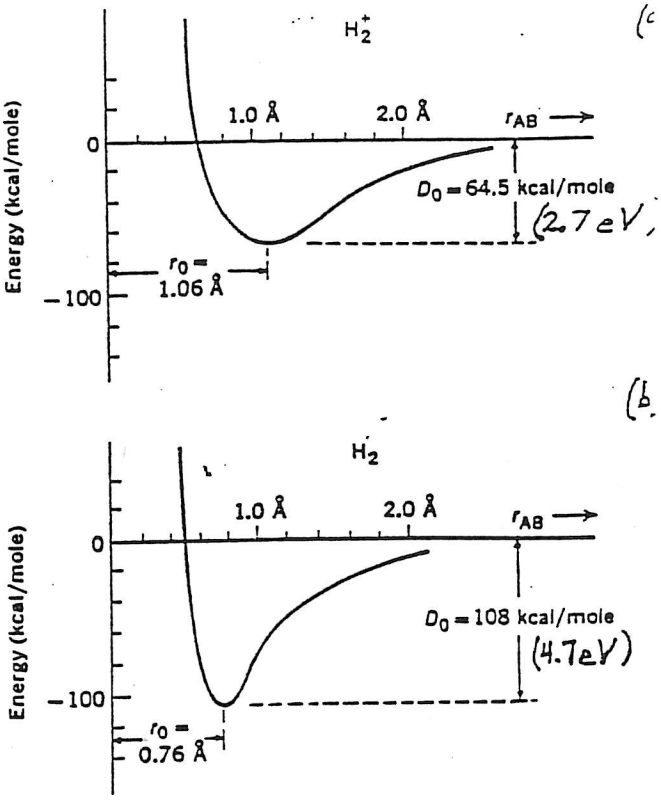

Figure 10 Energy versus internuclear distance for H_2^+ and H_2.

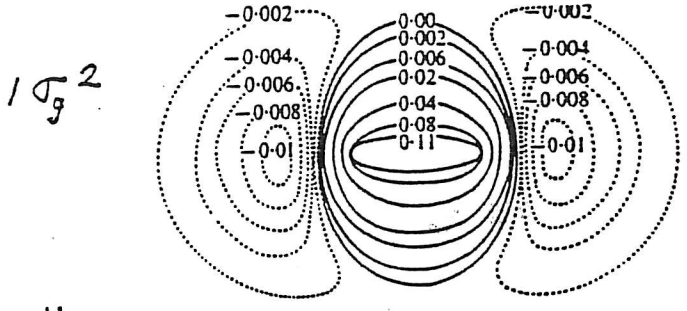

FIG. 11. Difference-density contours in H_2. The solid lines denote excess electron density; the dotted lines denote reduced density.

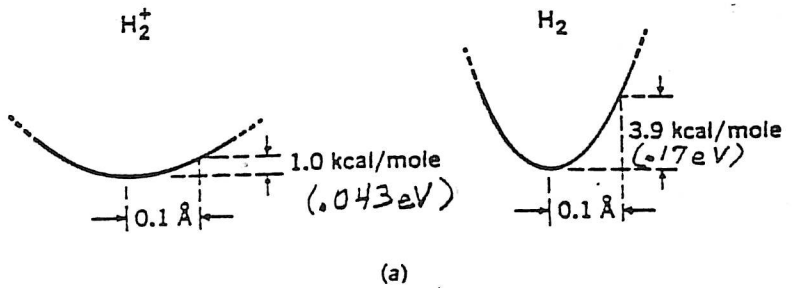

(a)

Figure 12 Molecular vibrations—a measure of bond order. (a) Greatly expanded view of the bottom of the energy curves of Figure 10 showing the energy required for a 0.1 Å change in bond length. (b) Ball-and-spring model shows a weak spring in H_2^+ and a stiff spring in H_2.

HOMONUCLEAR DIATOMIC MOLECULES
(Pi and Sigma Orbitals)

Just as we designate the ground-state electronic structure of atoms by their occupied AO's (H=1s, He=$1s^2$, Li=$1s^2 2s$, etc.), we designate the ground-state electronic structure of molecules by their occupied MO's ($H_2^+ = 1\sigma_g$, $H_2 = 1\sigma_g^2$).

We next consider the helium molecular ion, He_2^+. By the Pauli principle, the third electron cannot go into the $1\sigma_g$ bonding MO, so must occupy the $1\sigma_u^*$ anti-bonding MO, making its ground state $1\sigma_g^2 1\sigma_u^*$. With two bonding and one anti-bonding electrons, He_2 can be viewed as having a net bond corresponding to only one electron. It is therefore not surprising that the bond energy and bond length of He_2^+ are very similar to those of H_2^+. The neutral He_2 molecule would have a $1\sigma_g^2 1\sigma_u^{*2}$ configuration, and with two bonding and two anti-bonding electrons, would be expected to be unstable. It is.

Moving on to lithium, the 2s AO's will form $2\sigma_g$ and $2\sigma_u^*$ MO's in Li_2, which will have a ground-state configuration of $1\sigma_g^2 1\sigma_u^{*2} 2\sigma_g^2$. The K-shell electrons (two bonding, two anti-bonding, as in He_2) will provide no net bonding, and the splitting between $1\sigma_g$ and $1\sigma_u^*$ energy levels will be small, since the interatomic spacing will be determined primarily by the overlap of the 2s AO's, which are much larger. Since the $2\sigma_g$ bonding electrons of Li_2 are much further from the screened (by K-shell electrons) Li nuclei than the $1\sigma_g$ bonding electrons of H_2 are from the H nuclei, the bond energy of Li_2 is considerably lower than that of H_2.

A diatomic beryllium molecule would have a $1\sigma_g^2 1\sigma_u^{*2} 2\sigma_g^2 2\sigma_u^{*2}$ electronic configuration. With an equal number of bonding and anti-bonding electrons, the Be_2 molecule, like the He_2 molecule, is unstable.

Atoms heavier than Be have 2p electrons in the ground state. The building of MO's by the linear combination of p-type AO's can lead to MO's of different symmetries. Fugure 13 shows schematically the shape of bonding and anti-bonding MO's produced by 2s-2s overlap (Fig. 13a) and 2p-2p overlap (Fig. 13b), and now requires description of the traditional nomenclature for molecular orbitals. Orbitals that are unchanged by rotation about the molecular axis are designated sigma orbitals, and are numbered in order of increasing energy (1σ , 2σ , etc.) with asterisks often used to indicate anti-bonding orbitals ($1\sigma^*$, etc.). Sigma orbitals are formed by s-s overlap (Fig. 13a) and p_z-p_z overlap (Fig. 13b), where the z-axis is the molecular axis.

Orbitals that change sign on rotation about the molecular axis by half a turn, and have a nodal plane separating positive and negative lobes, are called pi orbitals. As with σ orbitals, they are numbered in order of increasing energy (1π , 2π, etc.) and asterisks usually are used to indicate anti-bonding orbitals ($1\pi^*$, etc.). As seen in Fig. 13c, p_x-p_x overlap and p_y-p_y overlap produce π orbitals. No MO's are produced by p_x-p_y, p_y-p_z, or p_z-p_x overlap, since, by symmetry, their net overlap integrals are zero.

Finally, the subscripts g and u (from the German - gerade, even, ungerade, odd) refer to another aspect of the symmetry of MO's. Orbi-

tals that are unchanged by inversion about the molecule's center of symmetry are labelled g; those that change sign on inversion are labelled u. As seen in Fig. 13, in a σ MO the bonding MO is σ_g, while in a π MO the bonding MO is π_u. Consistent with the arguments of the preceding section, the bonding MO's are those with the greater density of charge in the inter-nuclear region.

Adopting an "aufbau" approach to molecular structure, we need to know the energy sequence of the available MO's, as we did for the AO's of atoms in interpreting the periodic table. The sequence usually found is

$$1\sigma_g < 1\sigma_u^* < 2\sigma_g < 2\sigma_u^* < 1\pi_u < 3\sigma_g < 1\pi_g^* < 3\sigma_u^*$$

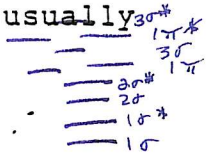

and the relation of the MO energies to those of the component AO's is seen in Fig. 14. As in H_2, overlap has led to a splitting of energy levels, with the bonding MO having a lower energy, and the anti-bonding MO a higher energy, than that of the component AO's. The degeneracy of the 2p AO's is partly broken, as the p_z AO's combine to form the $3\sigma_g$ and $3\sigma_u^*$ MO's (Fig. 13b) while the p_x-p_x and p_y-p_y overlaps produce doubly-degenerate $1\pi_u$ and $1\pi_g^*$ MO's (Fig. 13c).

An important point implicit in Fig. 14, and in the much simpler case of Fig. 6, is the conservation of the number of energy levels. In Fig. 6, the two 1s atomic energy levels (one on each nucleus) were transformed into two molecular energy levels, $1\sigma_g$ and $1\sigma_u^*$. In Fig. 14, the ten atomic energy levels (one 1s, one 2s, and three degenerate 2p levels on each atom) were transformed into ten molecular energy levels. This rule carries over to polyatomic molecules and into solids, where over 10^{23} atomic energy levels will lead to over 10^{23} energy levels in the solid.

With this nomenclature and background, we can now continue further into the periodic table and our consideration of homonuclear diatomic molecules. We can omit further discussion of the levels formed from 1s and from 2s AO's, which do not contribute to net bonding because electrons have filled an equal number of bonding and anti-bonding orbitals.

Our next candidate is boron, which has one 2p electron per atom. The B_2 molecule therefore has two electrons in the bonding $1\pi_u$ level, i.e., a $1\pi_u^2$ configuration. The two electrons form what chemists have traditionally called a single bond ("bond order" of one), as in H_2 and Li_2. However, moving to carbon, the C_2 molecule has a $1\pi_u^4$ configuration, the two electron pairs forming a double bond. Two nitrogen atoms form the N_2 molecule with $1\pi_u^4$ $3\sigma_g^2$, the net of six electrons (three electron pairs) forming a triple bond. This increase in bond order from B_2 to N_2 is accompanied by an increase in bond energy and force constant, and a decrease in bond length (Fig. 15).

Having filled all the available bonding MO's, further electrons must occupy anti-bonding states. Therefore in the oxygen molecule, two electrons occupy the $1\pi_g^*$ anti-bonding state, leading to a net of four (6-2) bonding electrons. Thus O_2 has a double bond. The F_2 molecule has four electrons in $1\pi_g^*$ and a net of only two (6-4) bonding

electrons, a single bond. The Ne_2 molecule, of course, is unstable. The trend across this row of the periodic table (Fig. 15) shows that the homonuclear diatomic molecule with the strongest bond is N_2, with a triple bond consisting of one sigma bond and two pi bonds.

An interesting aspect of the O_2 molecule is that the two electrons in the $1\pi_g^*$ state, by Hund's rule, go in with parallel spin, one occupying the MO formed from $2p_x$ and the other the MO formed from p_y (Fig. 16). Thus the MO picture shows that the O_2 molecule has a net magnetic moment, consistent with the experimentally-observed paramagnetic behavior of O_2.

For all the diatomic molecules discussed above, and others formed from heavier atoms, computer calculations using the LCAO and SCF methods have yielded bond strengths and bond lengths in good agreement with experiment. The only complication beyond the simplified discussion above is that the $1\pi_u$ and $3\sigma_g$ MO's have rather similar energies, and may reverse places in the energy sequence in some molecules, influenced by some mixture or "hybridization" of 2s and 2p AO's, an effect to be discussed in more detail later.

Historically, it was atomic spectra that led to our concept of quantized energy levels, the Bohr model, and our present wave-mechanical understanding of the electronic structure of atoms. Molecular spectra have also been widely studied, and provide quantitative evidence for the energy levels associated with molecular orbitals. Particularly useful has been photoelectron spectroscopy, in which molecules are subjected to monochromatic radiation whose photon energy $h\nu$ is sufficient to remove electrons from various energy levels. By measuring the distribution of kinetic energies of the emitted electrons, one can identify the energy levels associated with specific molecular orbitals. Figure 17 shows the photoelectron spectra of N_2, O_2, and NO molecules. The substructure within many of the peaks is associated with molecular vibrational energy levels, a complication that was not present in atomic spectra. Note that the peaks corresponding to 1s inner-shell electrons show nearly the same ionization energies as those of 1s electrons in isolated N and O atoms, as expected from the very limited overlap of these inner-shell AO's in the molecules.

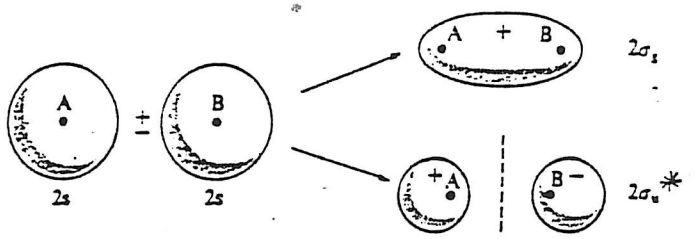

132

FIG. Combination of two 2s AO's to yield bonding and antibonding MO's (denoted by $2\sigma_g$ and $2\sigma_u^*$). The nodal plane is indicated by the broken line.

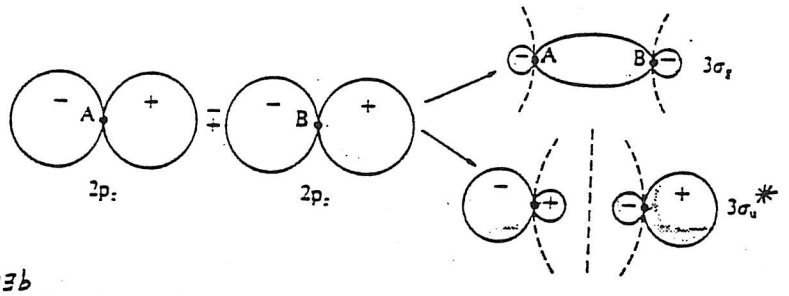

136

FIG. Combination of two $2p_z$ AO's to yield bonding and antibonding MO's (denoted by $3\sigma_g$ and $3\sigma_u^*$). The z axis is taken pointing to the right; note the signs on the lobes and the ways in which they combine. The nodal surfaces are indicated by broken lines.

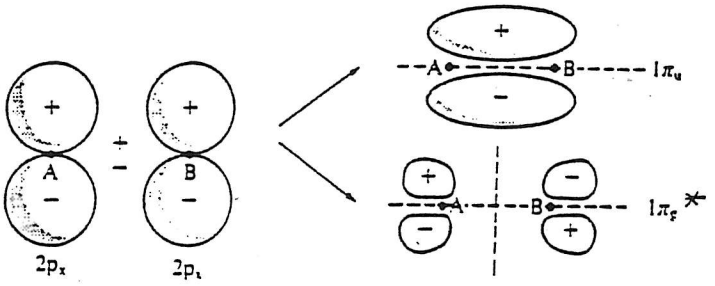

130

FIG. Combination of two $2p_x$ AO's to yield bonding and antibonding MO's (denoted by $1\pi_u$ and $1\pi_g^*$). x axis taken vertically. Note the signs on the lobes. The nodal surfaces are indicated by broken lines. Each MO is degenerate, its partner being similarly constructed from $2p_y$ AO's.

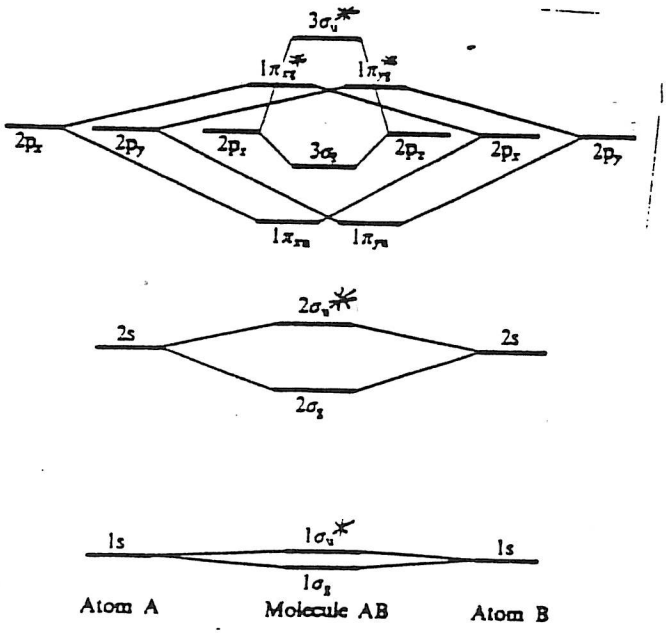

14

FIG. MO energy levels in a homonuclear diatomic molecule AB related to those of the separate atoms A and B (schematic).

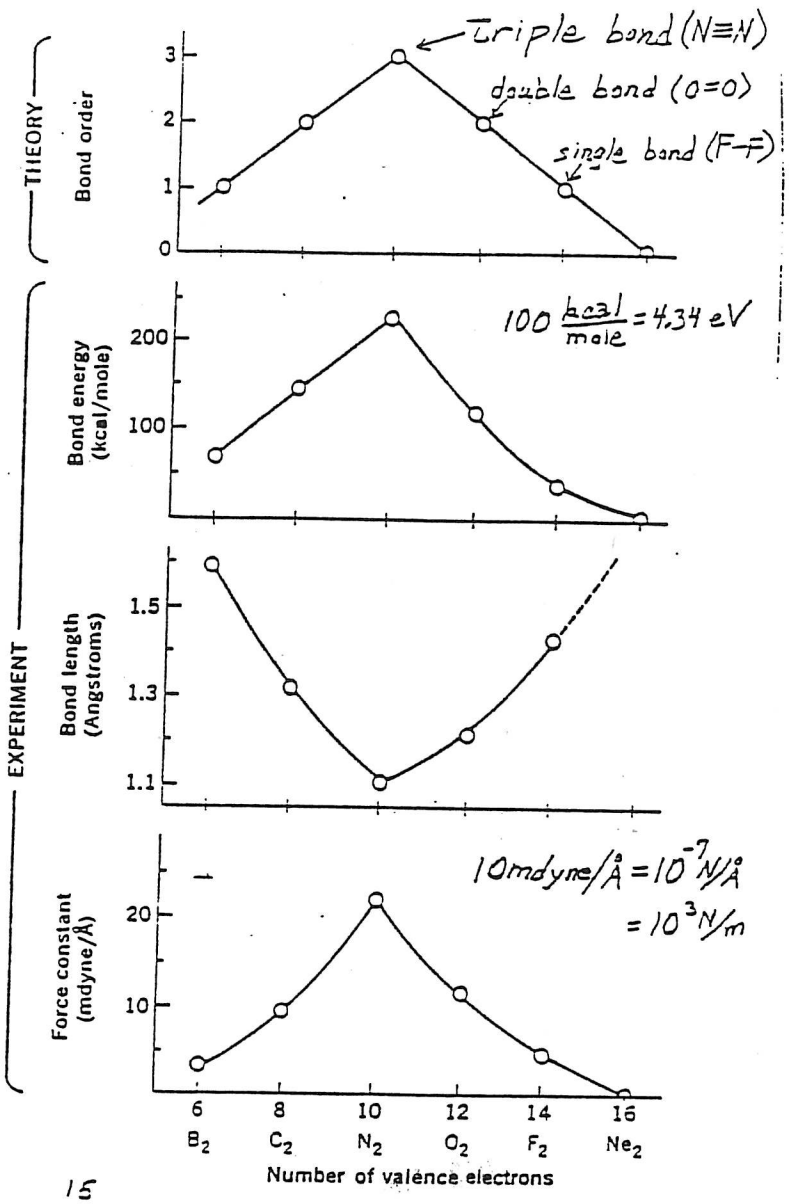

NOTE:
stronger bonds
are shorter
and stiffer

15

Figure — *Trends in bond properties and predicted bond orders in first-row homonuclear diatomic molecules.*

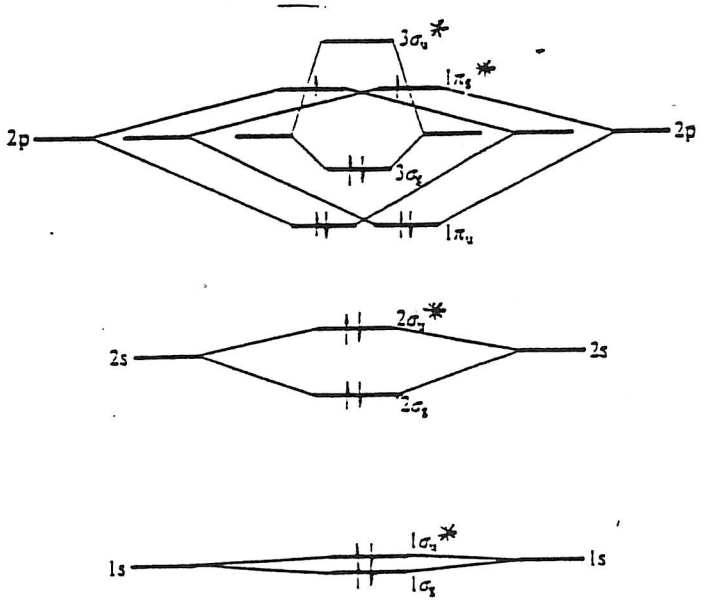

16

FIG. — Occupation of MO's in the molecule O_2. Energy levels for degenerate orbitals are shown separately (e.g. $1\pi_u$ includes the two MO's $1\pi_{xu}$ and $1\pi_{yu}$) and the spins of the electrons in the $1\pi_g$ pair are parallel coupled. The molecule is paramagnetic.

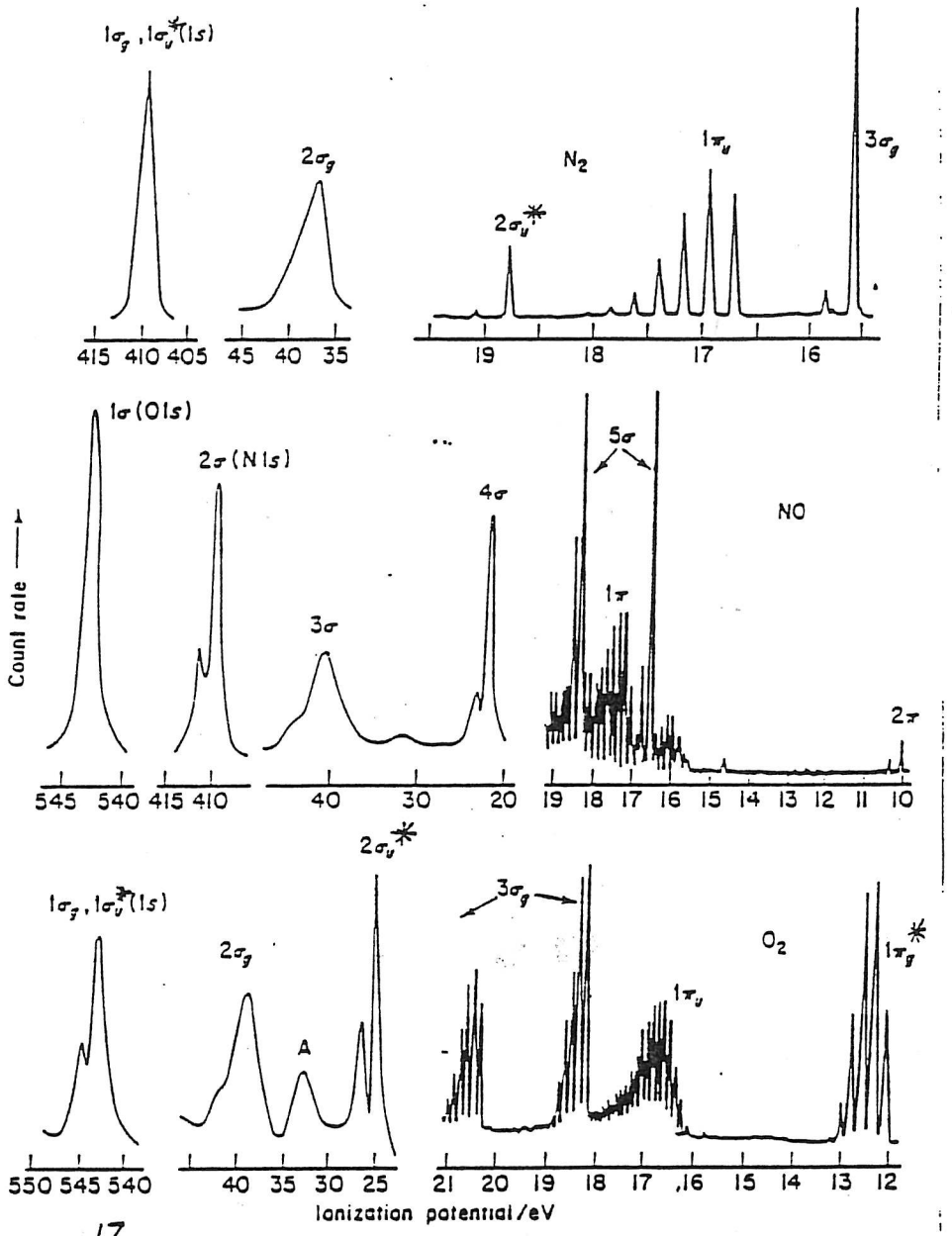

17

Figure [redacted] Photoelectron spectra of N_2, NO, and O_2. Spectra are shown as count rates (different scales for each segment of the spectra) against the ionization potential. The low ionization limits below 21eV were obtained with a HeI source (W. C. Price) and the region above with Mg $K\alpha$ irradiation (K. Siegbahn and coworkers). Fine structure in peaks from vibrational effects.

From SCF calculations, $E_{1s} = 408$ eV in the N atom, and 543 eV in the O atom. The 1s peaks in all three molecules correspond closely to these atomic levels, because the 1s AO's have little overlap, and are little affected by molecular formation. ($1\sigma_g = 1\sigma_u^*$) Notation of MO's for NO is different from the others because it is a heteronuclear molecule and lacks the symmetry of homonuclear molecules.

HETERONUCLEAR DIATOMIC MOLECULES
(Electronegativity)

In our discussion of homonuclear diatomic molecules, we considered only MO's built from matching AO's: $1s+1s \rightarrow 1\sigma$, $2s+2s \rightarrow 2\sigma$, $2p_z-2p_z \rightarrow 3\sigma$, and $2p_x-2p_x$ (and $2p_y-2p_y$) $\rightarrow 1\pi$. For heteronuclear molecules, we must consider other pairings of AO's. The choice of AO's is guided by three rules:

1. The AO's ϕ_1 and ϕ_2 must have the same <u>symmetry</u> relative to the molecular axis.
2. The <u>energies</u> of ϕ_1 and ϕ_2 should be as nearly matched as possible.
3. The AO's should have substantial <u>overlap</u>.

The first rule is demonstrated in Fig. 18. Fig. 18a shows the overlap of an s AO and a p_x AO (we continue to label the molecular axis as the z-axis). It is clear that areas of a negative product of the AO's will exactly balance those with a positive product, yielding a net overlap integral S_{12} of zero. On the other hand, an s AO can have a nonzero overlap with a p_z AO (Fig. 18b). Thus MO's can be built from s-p_z pairing, but not from s-p_x or s-p_y. Similarly, the symmetry requirement rules out forming MO's from p_z-p_x, p_z-p_y, or p_x-p_y overlap.

Both the first and second rules can be exemplified by consideration of the HF molecule. (We will delay discussion of the third rule until our discussion of polyatomic molecules.) The energy of the 1s electron of H is -13.6 eV, while the energies of the electrons of F are: 2p,-18.6 eV; 2s,-39 eV; 1s,-721 eV. By the energy criterion (rule 1), we can assume the bonding (and anti-bonding) MO's are built primarily from the 1s(H) and 2p(F) AO's. From the symmetry criterion (rule 2), we must choose $2p_z$ as the AO to bond the molecule. Six of fluorine's electrons will fill the 2s, $2p_x$, and $2p_y$ states in <u>nonbonding</u> orbitals, traditionally called "lone pairs" in chemistry. Two electrons will, of course, also fill the 1s "core" levels of F, their major role in the molecule being only to screen part of the nuclear charge.

Calculation of the bonding produced by the s-p_z overlap in HF will follow the same procedure outlined earlier for H_2^+. A MO is constructed as $\psi = c_1\phi_1 + c_2\phi_2$, the quantity $\mathcal{E}(\psi)$ is minimized, and the resulting secular equations are solved for c_1 and c_2 and the energies of the bonding and anti-bonding MO's. Figure 19 shows schematically how the results will differ from those of a homonuclear diatomic molecule. The energy level of the bonding MO will be below that of the lower of the two AO's (in this case, the $2p_z$ of F, -18.6 eV), and the energy level of the anti-bonding MO will be above that of the higher-energy AO (in this case, the 1s of H, -13.6 eV). Figure 19 also shows that the electron density of the bonding MO will be weighted towards F, the more electronegative atom, while the electron density of the anti-bonding MO will be weighted toward the H.

In the <u>homonuclear</u> diatomic molecule, when the two Coulomb integrals were equal ($H_{11}=H_{22}$), solution of the secular equations yielded (see p.9)

$$c_1 = \pm c_2 \qquad E = \frac{H_{11} \pm H_{12}}{1 \pm S_{12}}$$

Thus the MO's were symmetric ($c_1=c_2$) or antisymmetric ($c_1=-c_2$) and the splitting of the energy levels of the bonding and anti-bonding MO's was dominated by the bond integral H_{12}. In the heteronuclear diatomic molecul $H_{11} \neq H_{22}$, and solution of the secular equations yields a more complicated expression for the MO energy levels:

$$E = \frac{\{H_{11}+H_{22}-2S_{12}H_{12} \pm \sqrt{(H_{11}-H_{22})^2+4(H_{12}-S_{12}H_{11})(H_{12}-S_{12}H_{22})}\}}{2(1-S_{12}^2)}$$

For the case of a bond with highly ionic character, i.e., for $(H_{11}-H_{22})$ much larger than H_{12}, this simplifies to:

$$E = H_{22} - \frac{(H_{12}-S_{12}H_{22})^2}{(H_{11}-H_{22})} \qquad \text{(bonding MO)}$$

$$E = H_{11} + \frac{(H_{12}-S_{12}H_{11})^2}{(H_{11}-H_{22})} \qquad \text{(anti-bonding MO)}$$

so that in this case the energy gap between bonding and anti-bonding MO's is dominated by $H_{11}-H_{22}$, rather than by H_{12}.

In this limit, solving for c_2/c_1 yields:

$$\frac{c_2}{c_1} = -\frac{(H_{11}-H_{22})}{(H_{12}-S_{12}H_{22})} >> 1 \qquad \text{(bonding MO)}$$

$$\frac{c_2}{c_1} = \frac{(H_{12}-S_{12}H_{11})}{(H_{11}-H_{22})} << -1 \qquad \text{(anti-bonding MO)}$$

Thus the bonding MO is dominated by the lower-energy AO (electron transfer to the more electronegative atom) and the anti-bonding MO is dominated by the higher-energy AO (electron transfer to the less electronegative atom), as was shown schematically in Fig. 19.

Returning to the specific case of the HF molecule, the bonding MO will contain more of the $2p_z$(F) AO than of the 1s(H) AO. With two electrons occupying this MO, there will therefore be some effective transfer of electronic charge from H to F. If we simplistically assume a net charge of $-\delta e$ centered on the F nucleus and a net charge of $+\delta e$ centered on the H nucleus, this would yield a molecular dipole moment of $\delta e R_o$, where R_o is the internuclear spacing (the bond length). The quantity δ is commonly called the fractional ionic character of the bond. In HF, $\delta=0.43$, and the dipole moment is about 1.8 Debyes (where 1 Debye = 3.33×10^{-30} C-m).

In contrast, consider the molecule LiH. In this case, the 2s(Li) energy level is at -5.4 eV, much closer to the 1s(H) level than is the 1s(Li) AO, which at -65.3 eV is much too low to take part in the bonding. The bonding MO is therefore built between 2s(Li) and 1s(H). In this case, the electron density in the bonding MO will be weighted towards the 1s(H), which has the lower energy (Fig. 20). Thus in this molecule there is a net negative charge on the H, which, although less electronegative than F, is

more electronegative than Li. In LiH, δ=0.76, and the dipole moment is 5.9 Debyes. The LiH bond has a larger fractional ionic character than the HF bond. Electron density contours resulting from MO calculations for HF, LiH, and other first-row diatomic hydrides are shown in Fig. 21.

Finally, we consider the LiF molecule. Here the bonding MO is built from 2s(Li) and $2p_z$(F), and the resulting molecule has δ=0.84 and a dipole moment of 6.3 Debyes. The LiF bond is more ionic than either LiH or HF, reflecting a greater difference in electronegativities of the component atoms.

Pauling and others have devised systems to assign numerical values of electronegativity to each atom with the goal of predicting the fractional ionic character of chemical bonds (primarily as reflected by dipole moment and the ionic component of the strength of chemical bonds. For example, the strength of the LiF bond (5.9 eV) is far greater than that of the purely covalent bonds of Li_2(1.1 eV) or F_2(1.4 eV). By Pauling's formula, the difference between 5.9 eV and the geometric mean of 1.1 and 1.4 eV, or 5.9-1.2=4.7 eV, would be the ionic component of the bond energy, and would be proportional to $(\Delta n)^2$, the square of the difference in electronegativities of Li and F. However, correlations of Δn with fractional ionic character and bond strength have been found to be, at best, semi-quantitative guides for relative ionic character of bonds in specific series, such as hydrogen halides. As discussed in depth in Chapter 6 of Coulson's Valence, our present-day quantum-mechanical interpretation of chemical bonds makes it clear that no simple assignment of a single "electronegativity" number to each element can fully characterize the nature of its bonding to all other elements. However, through equations like those presented earlier, the LCAO-MO description of chemical bonding can quantitatively treat the continuum of bond types from purely covalent (H_2,N_2) through slightly polar (NO, CO) to predominantly ionic (LiH, LiF).

S-Pz
S≠0

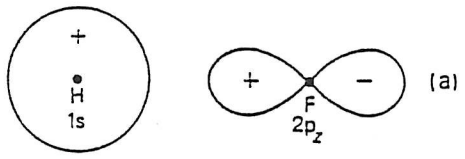

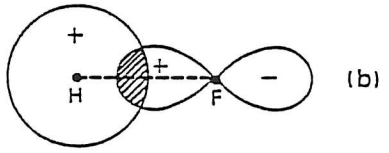

18b

Figure — Bond-forming AO's for HF: (a) separate AO's; (b) overlapped AO's.

S-Px
$S_{AB}=0$

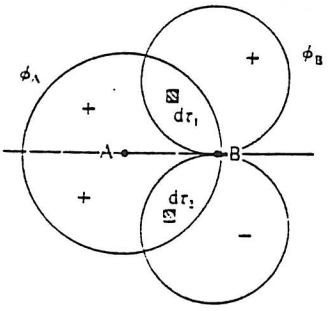

182

FIG. Overlap between orbitals of different symmetry type. Here ϕ_A is of s type, ϕ_B of p_x type, AB being taken as the z axis.

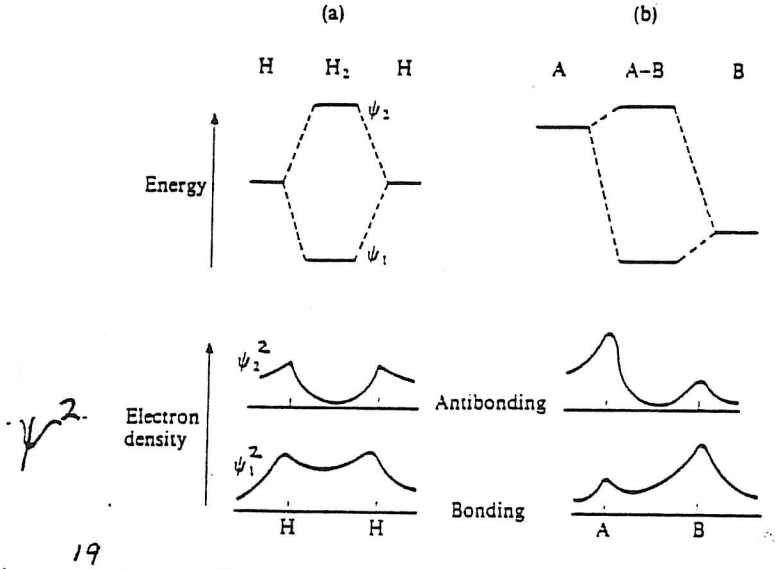

19

Fig. Electron distributions and energies of molecular orbitals in (a) H_2, and (b) a heteronuclear molecule AB.

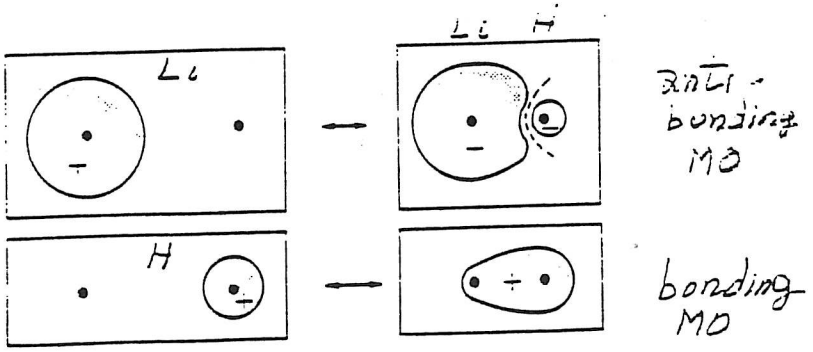

Fig. 20. Schematic mixing of s-orbitals of Li and H to produce asymmetric MO's.

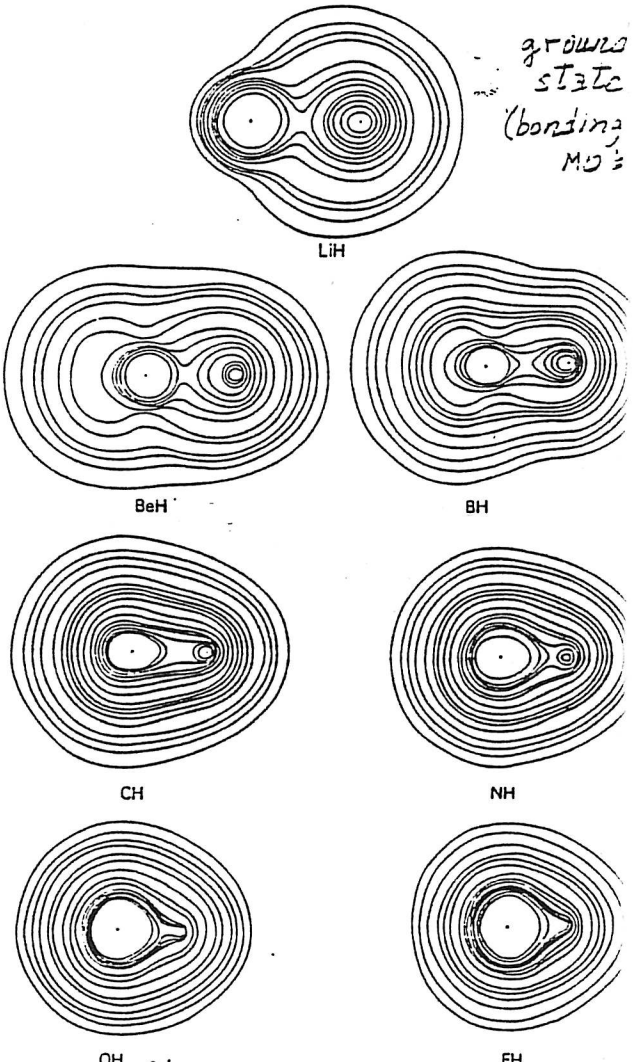

ground state (bonding MO's

21

Figure — Electron density contours for first-row diatomic hydrides (AH). All maps are drawn to the same linear scale. The nucleus A is on the left in each map, and its innermost contours have been omitted for the sake of clarity (after Bader, Keaveney and Cade, and reproduced by permission of the American Institute of Physics.

POLYATOMIC MOLECULES
(Hybridization)

In discussing diatomic molecules, we considered, for simplicity, only MO's built from one AO from each atom. In many cases, however, the combination of two or more AO's from the same atom can lead to MO's of lower energy through increased overlap. This concept of hybridizatio can make significant quantitative changes in MO calculations even in diatomic molecules, but plays a critical role in our understanding of the geometry of polyatomic molecules. (It is perhaps worthwhile at this point to remind ourselves that the LCAO approach is only an approximatic method for solving Schrödinger's equation for molecules. Use of more AO's, with adjustable coefficients, enables us to better approximate the "real" MO's, and thereby get a better approximation to the "real" energy levels.)

For example, Be forms linear BeX_2 molecules (X-Be-X) with X=H, Cl, Br, and I. This is difficult to understand in terms of the ground-state $1s^2 2s^2$ configuration of a Be atom. However, the 2s and 2p AO's of Be are fairly close in energy. If we were to construct hybrid AO's as $(\phi_{2s} + \phi_{2p_z})/\sqrt{2}$ and $(\phi_{2s} - \phi_{2p_z})/\sqrt{2}$, the resulting sp hybrids would extend further than either the 2s or 2p AO's, with their directions of maximum extent 180° apart (Fig. 22a). Each of these hybrids could overlap with a 1s(H) AO or a p_z orbital of Cl, Br, or I to produce a linear BeX_2 (Fig. 22b) molecule. The sp hybrid AO's are of higher energy than the 2s AO's (Fig. 23), but this is more than compensated for by the strong covalent bonds produced by increased overlap with the AO's of H or the halogens. Hybrids produced by equal mixing of s and p AO's are called digonal hybrids, and appear in linear molecules.

Analogously, bonding in the planar BH_3 molecule, which has three equivalent B-H bonds, is difficult to interpret in terms of the $1s^2 2s^2 2p$ ground-state electronic configuration of B. However, the mixing of one s and two p AO's can produce three sp^2 hybrids, with their directions of maximum extent at 120° to each other's (Fig. 24). As in BeX_2, the energy "cost" of hybridization is paid by the enhanced overlap and bonding. Each of the hybrids in BH_3 is produced by the mixing of one s and two p AO's, and such sp^2 AO's are called trigonal hybrids.

In CH_4 (methane) and numerous other molecules, carbon has four equivalent bonds arranged in tetrahedral symmetry, with an angle of 109.5° between bonds. These bonds are interpreted as arising from the overlap of 1s(H) AO's with sp^3(C) hybrids, constructed from one s and three p orbitals. Such hybrids are called tetrahedral hybrids (Fig. 25). Tetrahedral hybrids also account for the bonds in many organic compounds and in crystalline diamond, Si, and Ge.

In other molecules other percentages of s-p hybridization may produce minimum energy. In H_2O, for example, one MO model might use sp^3 hybridization, using two of the hybrids for bonding with the H atoms and the other two to accommodate the two lone pairs. Such sp^3 hybridization would predict a bond angle of 109.5° between the two O-H bonds. (A model based on no hybridization would predict 90°.) The experimental value is 104.5°. A model using 80%p and 20%s for the bonds with H, 60%s and 40%p for a lone pair in that plane, and pure p orbitals out of that plane for the other lone pair, has lower total energy than the sp3 model

and accurately predicts not only the experimentally-observed bond angle but also the experimentally-observed dipole moment. A similar model applied to NH_3, which has three equivalent N-H bonds and one lone pair, accurately predicts the experimentally-observed bond angle of 107°.

For molecules containing heavier atoms, hybrids containing d orbital (in addition to s and p orbitals) yield lower-energy MO's, and must be considered for full understanding of molecular geometries. For example, six sp^3d^2 hybrids, built from one 3s, three 3p, and two 3d AO's of S can explain the octohedral symmetry of SF_6. Figure 25 shows this and other local symmetries associated with hybrids containing d orbitals. For further discussion of polyatomic molecules in the LCAO-MO framework, see Coulson's Valence, Chapter 7.

Hybridization is particularly important in carbon compounds, which will be considered in more detail in the next section. Figure 27 shows the overlap integral S for two hybrids of form $s+\lambda p$ directed towards each other, at a fixed C-C internuclear distance, as a function of the percentage of s character. Whereas the overlap for pure p is 0.3, and that for pure s is less than 0.5, with hybridization the overlap can exceed 0.8. It is this increased overlap, and the resulting strengthening of the interatomic bond, that favors hybridization.

This figure indicates that overlap is greatest for sp hybridization, less for sp^2, and still less for sp^3. This suggests that sp bonds should be stronger than sp^2 bonds, which in turn should be stronger than sp^3 bonds. The following table showing data for C-H bonds in various molecules supports this view.

Properties of CH bonds involving different hybridization

Hybridization	Molecule	C—H bond length (nm)	Stretching force constant ($N\,m^{-1}$)	Approximate bond energy ($kJ\,mol^{-1}$)	
sp	Acetylene (C_2H_2)	0·1061	639·7	500	5 eV
sp^2	Ethylene (C_2H_4)	0·1086	612·6	440	4.4
sp^3	Methane (CH_4)	0·1093	535·7	411	4.1
(p)	CH radical	0·1120	449·4	330	3.3

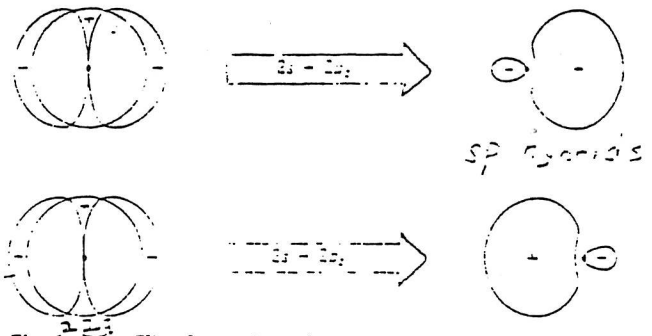

Fig. The formation of two digonal *sp* hybrids. In general, the combination of the *ns* and an *np* AO of the same atom produces two *sp* hybrids with their directions of maximum extent 180° apart.

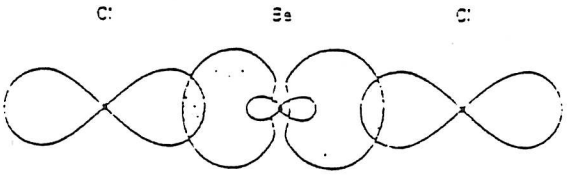

22b

Fig. Schematic diagram of the overlap of two Cl *3p* atomic orbitals with the Be *sp* hybrid orbitals to form linear $BeCl_2$.

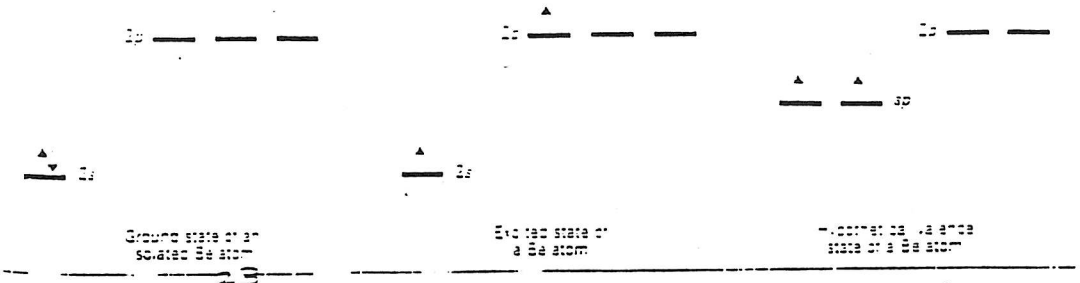

Fig. 23. Energy level diagram for beryllium comparing the ground state with the valence state used to form two covalent bonds. In the valence state there are two unpaired electrons in the two *sp* hybrid atomic orbitals. Note that there are always four atomic orbitals. The 2*s* and one of the 2*p* orbitals have been replaced by two *sp* hybrids.

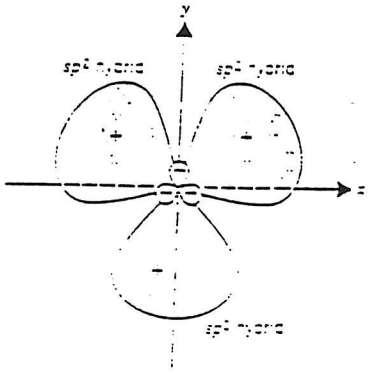

Fig. 24. The formation of three equivalent sp^2 trigonal hybrids with maximum extent in the *xy* plane by linear combination of the *s*, p_x, and p_y atomic orbitals. The directions of maximum extent of these three sp^2 hybrids are at 120° to one another. The geometry of a molecule in which the central atom uses these sp^2 hybrids is trigonal planar.

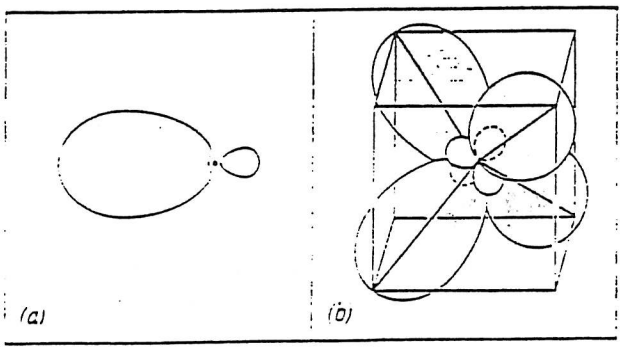

Fig. 25. (a) Electron density distribution in an sp^3 tetrahedral hybrid AO. (b) The four sp^3 tetrahedral orbitals showing their relative orientations in space.

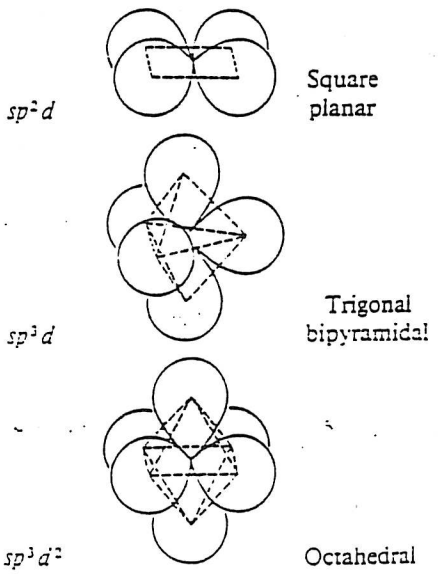

Fig. 26

Symmetries associated with hybrids containing d orbitals

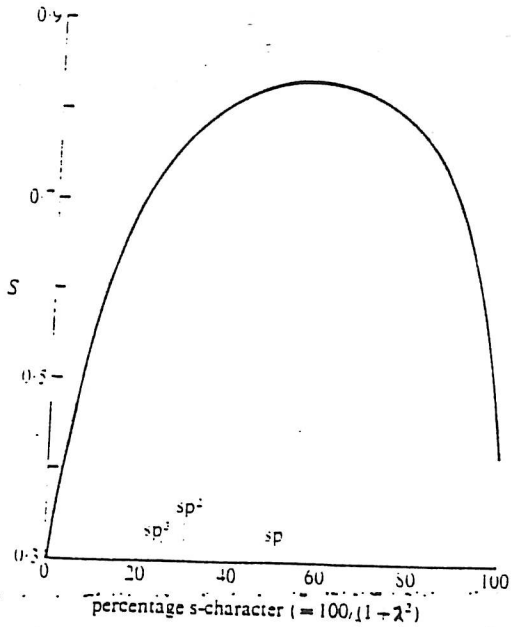

FIG. 27. Dependence of overlap on hybridization parameter λ for two hybrids in a C—C bond at fixed internuclear distance.

CARBON COMPOUNDS
(Delocalization)

The whole field of organic chemistry, including poymers and biological molecules, derives from the bonding versatility of the carbon atom. The three main types of C-C bond, in all of which carbon exhibits its normal quadrivalence, are: the single bond, as in ethane, the double bond, as in ethylene, and the triple bond, as in acetylene.

In ethane (C_2H_6), each carbon atom has one C-C bond and three C-H bonds in nearly tetrahedral symmetry, with bond angles approximately 109.5° (Fig. 28). Bonding is interpreted in terms of sp^3 hybrids, the C-C bond based on sp^3-sp^3 overlap, the C-H bond on overlap of carbon sp^3 hybrids with 1s AO's of H. All bonds are single (one electron pair) and of σ type. All other hydrocarbons of the alkane (C_nH_{2n+2}) series - propane, butane, pentane, etc. - contain only single bonds. Molecules in which each carbon atom forms four single bonds of essentially σ type are called saturated compounds.

In ethylene (C_2H_4), the molecule is planar, with bond angles near 120° and bonding interpreted with sp^2 trigonal hybrids. Each carbon has three in-plane σ bonds (one C-C, two C-H), but the 2p electron remaining on each carbon participates in a π bond (Fig. 28). The C-C bond is thus double, with one σ bond and one π bond. Molecules like ethylene in which one or more carbon atoms have multiple bonds, and are bonded to less than four atoms, are called unsaturated compounds. Ethylene can serve as a monomer for polymer formation. Breaking the double bond and attaching an extensive series of CH_2 groups yields polyethylene (Fig. 29) Polyethylene contains only single bonds and therefore is saturated.

In acetylene (C_2H_2), the atoms are collinear, and the appropriate hybridization is digonal (sp). Each carbon atom has two σ bonds (one C-H, one C-C) and has two additional 2p electrons available for π bonding. Therefore the C-C bond is a triple bond, consisting of one σ bond and two π bonds, as in the N_2 molecule (Fig. 30).

Acetylene can serve as a monomer for polyacetylene, a polymer in which conventional structural formulas show alternate single and double bonds (Fig. 31). Such molecules are termed conjugated compounds. The energy levels associated with π-type MO's in many conjugated compounds are close enough to lead to absorption in the visible part of the spectru and hence such molecules are colored. An example is indigo, commonly use to color blue jeans. (Chapter 6 of The Physics and Chemistry of Color by Kurt Nassau contains an interesting discussion of organic colorants, both natural and man-made, in terms of the energy levels of π-type MO's. Indigo, like many colorants, contains conjugated rings of carbon atoms. The prototype conjugated ring molecule is benzene (C_6H_6). Consideration of the MO structure of benzene and other conjugated organic compounds leads to the concept of delocalization.

In most polyatomic molecules, bonding can be described in terms of MO's that are essentially localized on individual bonds. This approach, however, breaks down completely for conjugated compounds. The prime example is benzene, for which diffraction and spectroscopic evidence show that the six carbon atoms form a regular plane hexagon, with 120°

bond angles and six equivalent C-H and C-C bonds. This implies trigonal sp^2 hybridization at each carbon atom, with the C-H and C-C bonds formed by overlapping AO's to give localized σ bonds.(Fig. 32). However, there are 6 electrons remaining to be accounted for, the 2p unhybridized AO's on each carbon atom directed out of the plane (Fig. 33a). These can be paired in various ways to form three localized π bonds (Fig. 33b&c), but since all six bonds are known to be equivalent, it was earlier assumed that the molecule "resonated" between such forms. However, by MO theory, we interpret the electronic structure of the benzene molecule differently. We assume a <u>delocalized</u> MO extending over the entire molecule, constructed as

$$\psi = c_1\phi_1 + c_2\phi_2 + \cdots + c_6\phi_6$$

where $\phi_1, \phi_2 \cdots \phi_6$ are 2p AO's centered on each of the six C atoms. Following the LCAO approach, we minimize $\mathcal{E}(\psi)$ and solve the secular equations for c_j and the energy levels of the six MO's - three bonding and three anti-bonding. The lowest-energy bonding MO has all c_j equal, and consists of two doughnut-shaped lobes of opposite sign (Fig. 34). The calculations show that this delocalized MO has a lower energy than the localized MO's shown in Fig. 33b&c. The difference is called the <u>delocalization energy</u> (or, for historic reasons, the resonance energy).

More generally, this approach can be used for any conjugated chain or ring molecule (Fig. 35) by an approximation method originally introduced by Hückel in 1931. The actual potential energy function V that is experienced by each π electron is rather complex, arising from the nuclei and core electrons, the localized σ bonds, and an average field due to the charge distribution of the other π electrons (using the SCF approach). Rather than completing the full calculation, Hückel introduced a semi-empirical approach, in which the unknown quantities are chosen so that the results fit a few typical molecules, and then are used to predict results for other molecules. He made the following approximations:

1. All Coulomb integrals $H_{jj}=\alpha$.
2. All bond integrals $H_{ij}=\beta$ for adjacent atoms, and are zero otherwise.
3. All overlap integrals $S_{ij}=0$. (This will obviously affect the quantitative results, but not the qualitative picture.)

With these approximations, solution of the secular equations for a chain of N conjugated carbon atoms yields for the energy levels of the N MO's:

$$E_k = \alpha + 2\beta \cos\left(\frac{k\pi}{N+1}\right) \qquad (k=1,2,\ldots.N)$$

(Note that for N=2, k=1 and k=2 correspond to $E=\alpha \pm \beta$, corresponding to our earlier solution for diatomic molecules if you take $S_{12}=0$.)

Thus there are N levels, symmetrically disposed about α (Fig. 36) The lower energy levels correspond to bonding MO's, the higher energy levels to anti-bonding MO's. (For odd N, one level will have $E=\alpha$, corresponding to a non-bonding MO.) The spacing between energy levels decreases with increasing N, leading to energy absorption at lower

energies. As the chain becomes longer and longer, we obtain an almost continuous band of energy levels of width 4β. The lower half of the band corresponds to bonding MO's, the upper half to anti-bonding MO's.

Similarly, one can apply the Hückel approximation to a conjugated ring of N atoms. Here the solution must be cyclic, so that $c_{N+1}=c_1$. Solution of the secular equations yields

$$E_k = \alpha + 2\beta \cos\left(\frac{2k\pi}{N}\right) \qquad \left(k = 0, \pm 1, \pm 2, \ldots \frac{N}{2}\right)$$

Again there are N levels, symmetric about α only for even N (Fig. 37). All but the lowest energy level (and the highest for even N) are doubly degenerate. For benzene (N=6), for example, the lowest energy level (k=0) corresponds to the bonding MO shown in Fig. 34. In the ground state, the six π electrons of benzene will occupy this MO and the two doubly-degenerate bonding MO's of higher energy ($k=\pm 1$). For large N, as for the conjugated chains, there will be an almost continuous "energy band" of width 4β. In the ground state, the N delocalized π electrons will occupy the N/2 energy levels corresponding to the bonding MO's, i.e., the band will be half-filled.

For both the chains and the rings, the delocalization of the wave functions has led to a spreading of the atomic energy level (α) into an energy band. This is analogous to the development of atomic energy levels into energy bands in crystals, and a long chain or ring can be viewed as a one-dimensional "crystal".

The general form of the delocalized wave functions corresponding to the energy levels in Figs. 36 and 37 can be seen from the coefficients c_j of the AO's making up the MO's ($\psi_k = \sum_j c_j^k \phi_j$). For the chains, the coefficient c_j^k (the jth coefficient for the kth MO) is, except for a normalization constant, given by $\sin\left(\frac{\pi j k}{N+1}\right)$

Viewed as a continuous function of j, this represents standing sine waves of 1/2, 1, 3/2, ...N/2 wave lengths along the chain, for k=1,2,3,...N. By themselves, these sine waves are solutions of Schrödinger's equation for an electron in a one-dimensional box with infinite walls. Multiplied by a 2p AO centered on each carbon atom, they correspond to the MO's, the lower energies corresponding to longer wave lengths (lower k's).

For the rings, the coefficients c_j^k are proportional to $e^{i(2\pi jk/N)}$

and, viewed as a continuous function, correspond to traveling waves, with opposite signs of k corresponding to waves traveling about the rings in opposite directions (yielding doubly-degenerate levels). These wave functions correspond to the Bloch waves we will encounter later in the course, when we deal with wave functions in crystals.

The difference between the solutions for chains and rings arose because of different "boundary conditions" we imposed on the c_j. For the rings, we took $c_{-1}=c_{N-1}$, often called "periodic boundary conditions", while for the chain we implicitly took $c_{N+1}=c_0=0$, equivalent to boundary conditions for a one-dimensional box with infinitely high walls.

Later in the course, we will develop energy bands in solids from a different viewpoint, that of nearly-free electrons. However, it can be seen from our treatment of conjugated molecules that crystal orbitals (CO's) and associated energy bands can be developed from the LCAO approach.

* * * * *

An interesting example of a crystalline conjugated system is graphite, which has a hexagonal layer structure (Fig. 38a). Within the layer planes, the carbon atoms are bonded with σ bonds formed from sp^2 trigonal hybrids, and with delocalized π electrons formed from 2p AO's normal to the plane. The delocalized π electrons give graphite metal-like conductivity parallel to the layer planes. Between the layers, there are only weak van der Waals forces, and much lower conductivity. In contrast, carbon in diamond (Fig. 38b) is bonded with four localized σ bonds from sp^3 tetrahedral hybrids, and diamond is an insulator.

SUMMARY

The LCAO-MO-SCF approach to chemical bonding is capable of calculating approximate electronic wave functions and associated energy levels that, with sufficient terms and computer time, are consistent with experimental spectroscopic data. Even with homonuclear diatomic molecules, such calculations also yield results on molecular properties that are forerunners of the properties of solids - bond length (lattice parameter), force constant (elastic modulus), quantized molecular vibrations (phonons) and bond energy (cohesive energy). With heteronuclear diatomic molecules, results on dipole moments also appeared. Consideration of polyatomic molecules led to conclusions on molecular geometry, a forerunner of crystal symmetries. Finally, consideration of carbon compounds led to the concept of delocalized wave functions and, for large molecules, associated energy bands, a forerunner of the energy bands of solids that are important in understanding electrical, magnetic, and optical properties.

For some properties of some solids, the LCAO method is the best starting point. For others, the nearly-free electron model may be the best starting point. A versatile materials scientist or engineer should have some familiarity and ease with both approaches.

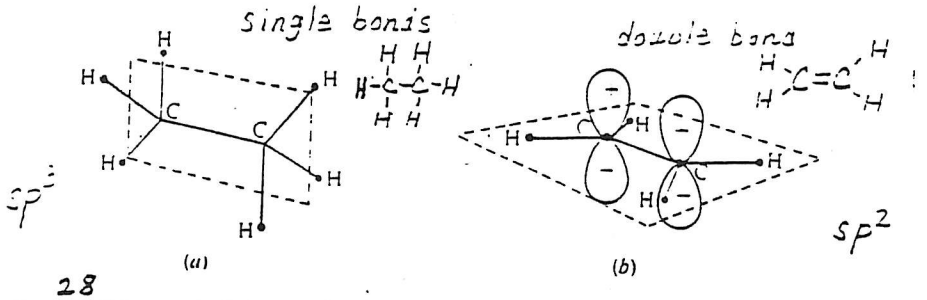

28

FIG. [redacted] Ethane and ethylene. (*a*) In ethane each carbon is in a tetrahedral valence state forming four σ bonds. The conformation is 'staggered', diagonally opposite CH bonds lying in the plane indicated. (*b*) In ethylene each is in a trigonal state, forming three σ bonds. The remaining electrons provide a π bond whose MO, formed by overlap of the 2p AO's shown, is antisymmetric across the molecular plane.

in polyethylene (or 'polythene') the monomer, ethylene

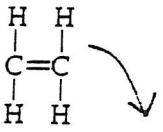

is joined many thousands of times into the polymeric chain

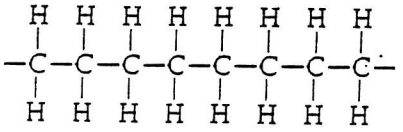

which may be written more simply as

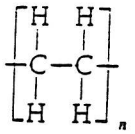

Fig. 29

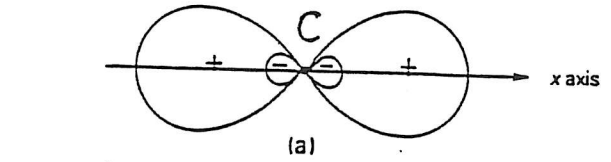

SP

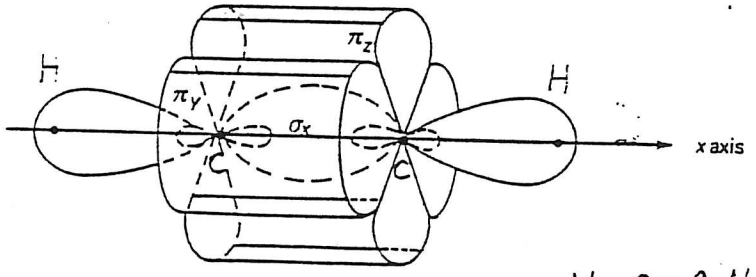

H-C≡C-H

30-Acetylene

Figure [redacted]: (a) Linear sp carbon hybrid orbital, (b) the $2p_y$ and $2p_z$ AO's are mutually perpendicular with the x axis, [redacted] σ and two π MO's in C_2H_2. (Triple bond)

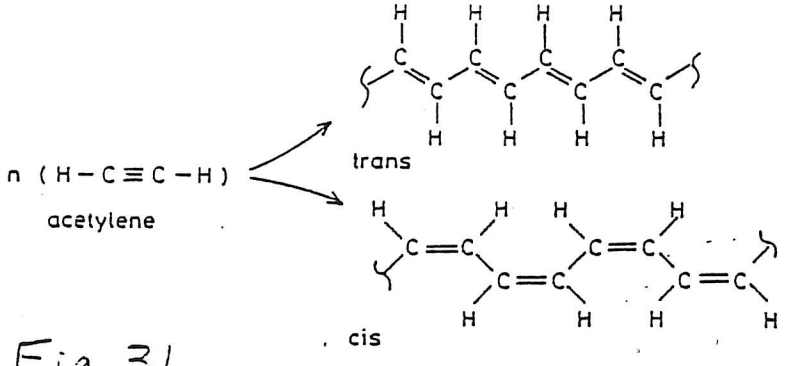

Fig. 31

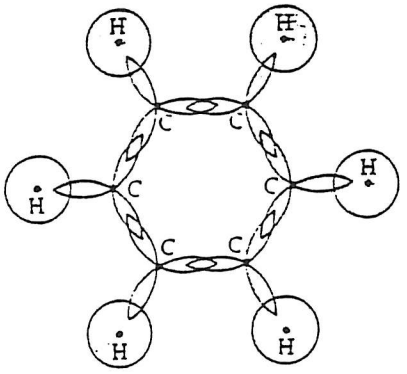

sp^2

32

FIG. [redacted]. Construction of σ bonds in the benzene molecule (the carbon hybrids have been highly stylized for clarity).

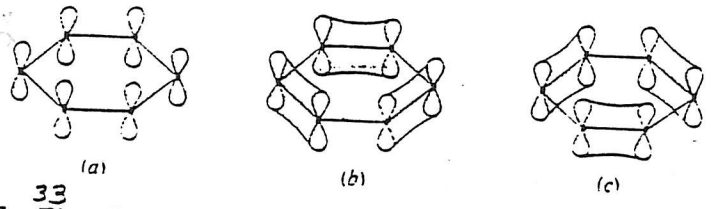

FIG. 33 (a) The π-type AO's in benzene and (b, c) two Kekulé pairing schemes.

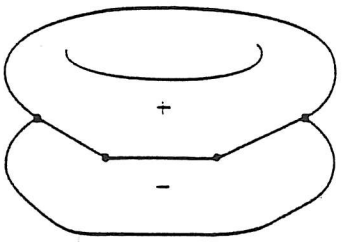

FIG. 34. Form of the lowest-energy bonding MO of π type in benzene. (This is *one* MO with two 'doughnut-shaped' lobes separated by a nodal plane which contains the carbon atoms.)

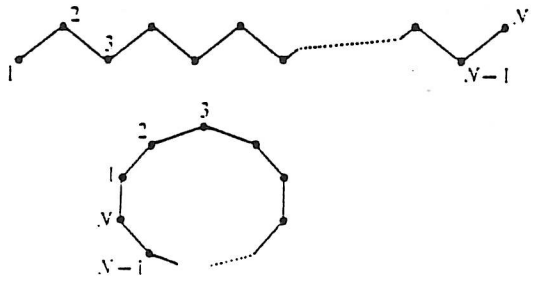

FIG. 35. Conjugated chains and rings. All molecules are assumed to be planar. Each atom has one π-type AO, $\varphi_1, \varphi_2, \ldots, \varphi_N$.

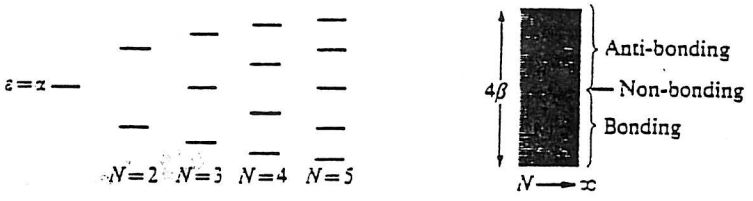

FIG. 36. Distribution of energy levels for a conjugated chain of N atoms. As N increases the levels become closer and closer, forming an 'energy band' of width 4β.

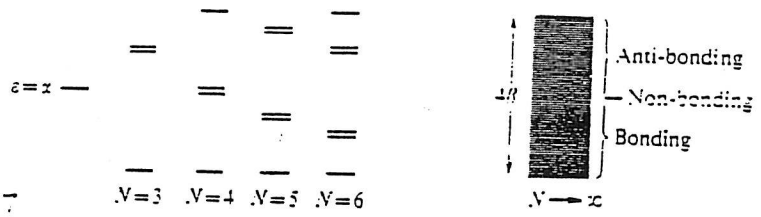

FIG. 37. Distribution of energy levels for a conjugated ring of N atoms. All the levels in the band are doubly degenerate except the lowest and, for N even, the highest.

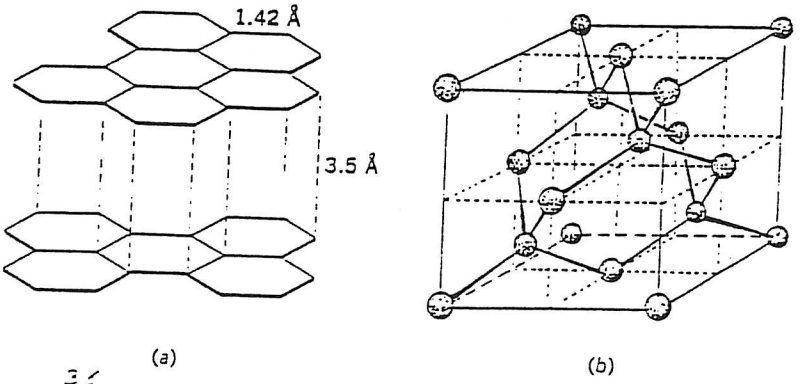

Figure 38 Carbon structure: (a) graphite, showing fragments of two adjacent layers; (b) diamond.